

Contents lists available at ScienceDirect

# Nano Trends

journal homepage: www.elsevier.com/locate/nantre





# Electrochemical epitaxy of nanostructures

Yuwei Guo<sup>a,\*</sup>, Yang Hu<sup>a,b</sup>, Jian Shi<sup>a,b,\*</sup>

- <sup>a</sup> Department of Materials Science and Engineering, Rensselaer Polytechnic Institute, Troy, NY 12180, USA
- <sup>b</sup> Department of Physics, Applied Physics, and Astronomy, Rensselaer Polytechnic Institute, Troy, NY 12180, USA

ARTICLEINFO

Keywords: epitaxy electrochemical nanostructures

#### ABSTRACT

Epitaxy of nanostructured materials is a critical step in developing functional nanodevices. Electrochemical epitaxy has been shown robust and low-cost in advancing the deployment of nanomaterials. This paper offers a brief review on a wide category of nanostructured materials and phases synthesized via electrochemical epitaxy approaches over the past several decades. The review highlights the advantages of electrochemical approach over other high-temperature, high-vacuum technologies in terms of accessibility to target materials' phases, morphologies and yield. Electrochemical epitaxy's extraordinary ability in enabling certain valence states which cannot be reached at vacuum condition could bring new concepts in developing a plethora of metastable functional materials. It also gives an overview on possible growth modes and mechanisms that may be employed in developing emerging materials and phases.

## Introduction

In the past decades, epitaxy has attracted significant amount of interest due to its ability to obtain high quality crystalline materials for either device application or fundamental studies of materials physics on atomic-scale materials. Several methods have been developed to achieve epitaxial growth, such as physical vapor deposition, chemical vapor deposition, molecular-beam epitaxy, pulsed-laser deposition, to name a few. However, these vacuum-based techniques are relatively expensive and require high operation temperature to achieve adequate atom diffusion on the substrate surface which is essential for generating high quality materials.

This review is focused on electrochemical epitaxy approach for the development of nanostructures which can be carried out at low temperature and ambient pressure.

On the contrary, electrochemical deposition enables low-temperature deposition, which simplifies equipment design and fabrication costs, and also enables organic materials (e.g. PTFE) deposition and employment of thermally and chemically sensitive substrate like plastics [1]. Within the aqueous electrochemical deposition temperature range (from room temperature to 100 °C), researchers have observed increasing solution temperature helps improve crystallinity [2–4]. Higher solution temperatures also contribute to reduced gas content impurities in deposits [5–8].

Besides, electrochemical deposition offers more degrees of freedom

in terms of manipulating experimental variables. For instance, the deposition potential, which controls the energy barrier of cell reactions; the current, which controls the deposition rate, and thus, film morphology; deposition temperature, electrolyte components and pH values can all be manipulated during electrochemical deposition and give rise to an optimal growth condition for the target material. Electrochemical deposition can also be used to prepare non-equilibrium materials or crystal structure that cannot be accessed by other processing means.

Electrochemical deposition also has the advantage of providing a more conformal and higher rate deposition, and is easier to scale up for large surface area deposition. Compared to more compact structure with crystallites touching each other obtained in sputtering, electrodeposited films consisting of larger grains and bigger voids exhibit lower interface residue stress [9]. In addition, electrodeposition offers the possibility of defect passivation in a wet chemical environment. For example, the CdCl<sub>2</sub> treatment of CdS/CdTe solar cells is known to enhance efficiency values significantly [10]. Although the scientific understanding of this process is not fully agreed upon, it likely involves grain growth, doping, and defect passivation during the wet treatment and annealing process. Electrochemical deposition stands out as a versatile and valuable technique for material growth, offering benefits such as phase control, passivation mechanisms, and opportunities for scientific exploration and materials development.

Electrochemical deposition has its own shortcomings. Since the

<sup>\*</sup> Corresponding authors at: Department of Materials Science and Engineering, Rensselaer Polytechnic Institute, Troy, NY 12180, USA. *E-mail addresses*: guoy10@rpi.edu (Y. Guo), shij4@rpi.edu (J. Shi).

substrate serves as the working electrode, it needs to be conductive. Due to the requirement of maintaining the conductivity of working electrode during deposition, there is limited deposition thickness for insulating films [11]. Electrochemical deposition also has the limitation due to its "wet" plating predominantly taking place in aqueous solutions, which may introduce  $H^+$  ions into substrate or coating, leading to hydrogen embrittlement. Generation of hazardous substances and wastewater is another drawback of electrochemical deposition comparing to vapor deposition [12].

Similar to vapor deposition techniques, proper deposition conditions need to be selected in electrodeposition to get correct phase the desired crystallinity. Relations between structures of electrodeposits and deposition conditions such as current density, inhibition, metal ion concentration, addition agents, temperature, agitation and polarization have been reported (Fig. 1) [13,2].

Use chromium deposition as an example [14], chromium deposits obtained by electrochemical deposition show more pores and cracks than that deposited by sputtering. This can be explained by the high substrate temperature used in sputtering which gives more energy for atoms to move on substrate and fill in pores and cracks to reach a lower energy structure. The lower solution temperature also leads to a higher gas content impurity such as O, N, H, S moving from solution into deposits [5–8]. Similarly, when comparing electrochemical deposited and vapor deposited copper films, electroplated film has about 30 % higher resistivity than vapor deposited one due to more defects such as twins, more grain boundaries (small grain sizes), and higher dislocation density [3,4]. The annealing of the Cu film does help to increase atom diffusion to eliminate those structure defects and increase film resistivity to its bulk value. A list of advantages and disadvantages is displayed in Fig. 2.

The basic setup of electrodeposition system is shown in Fig. 3. It is a three-electrode cell, containing working electrode, counter (auxiliary) electrode, and reference electrode. Working electrode is the electrode under investigation during the electrodeposition. It can be connected to either anode or cathode, depending on whether oxidation or reduction reaction is expected to happen on this electrode. In experiments, working electrode is usually designed to have a certain surface area, for instance, 100 cm², so current density during deposition can be calculated, which is more meaningful than reporting a current value. The counter electrode is essential to complete the current flow circuit between anode and cathode. Basically, it can be any conductive material that does not introduce contaminants into electrolyte. Once we have

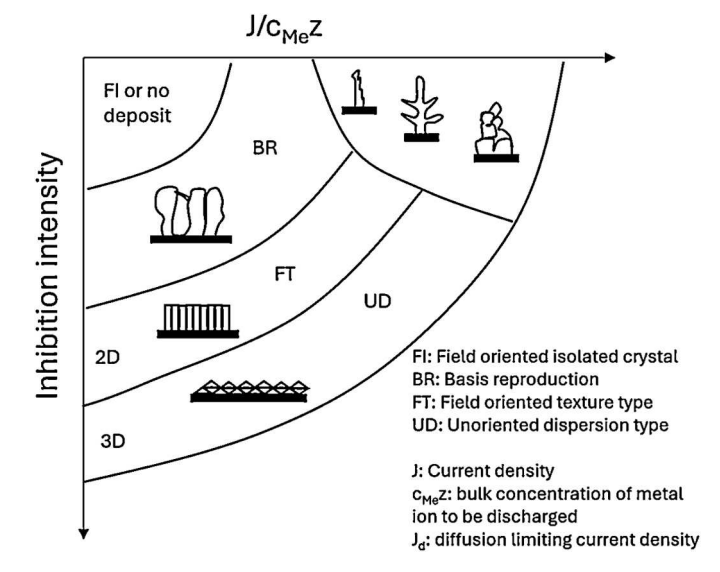


**Fig. 1.** Possible morphologies of crystals by electrochemical deposition. (Adapted with permission from *Electrochimica Acta*, 39 (1994) 1091.).

working electrode and counter electrode, the electrochemical deposition can already be conducted. However, a third electrode, reference electrode, is generally involved. The reference electrode serves as a stable potential reference so that we can measure the potential of working electrode relative to the reference electrode. Reference electrode does not participate in the cell reactions and it carries no more than the most negligible current. Thus, the reference electrode almost does not develop over potential during the electrochemical deposition, and functions as an unchanged potential reference point for working electrode. The reference electrode should be placed close to the working electrode. This will improve the accuracy of measuring working electrode potential relative to the reference electrode potential by reducing the percentage of measured potential contributed by the electrolyte between working electrode surface and reference electrode. During deposition, Redox reactions taking place near electrodes are promoted by extracting and providing electrons from and to anode and cathode, respectively, by external power supply. For instance, Fig. 3 shows electrochemical synthesis of KBiO<sub>3</sub> crystal. Bi<sup>3+</sup> ions are provided by the electrolyte and are oxidized to Bi<sup>5+</sup> ions, and reduced to Bi metal at anode and cathode, respectively. Outside the electrolyte, current is carried out by electrons in the external circuit while inside the electrolyte, current is carried out by ions. So electrolyte needs to be ionic conductive [15]. Besides, when choosing electrolyte, one needs to make sure that the electrolyte does not contain ions that involve side cell reactions at the deposition range of desired material.

When investigating growth conditions for a target material, Pourbaix diagram plays an important role. It gives information on the potential and electrolyte pH ranges for the stable existence of a certain material. Pourbaix diagram to electrochemical deposition is as the phase diagram to vacuum-based deposition methods. A well-established pourbaix diagram for CdTe system is shown in Fig. 4 [16]. It provides guideline for choosing deposition potential and electrolyte pH values for electrochemical deposition of CdTe thin films.

The growth modes associated with electrochemical deposition are studied by many research groups for a wide range of materials (Table 1). It seems that generally there is no unique growth mode compared to other epitaxial thin film growth strategies. Depending on the relative strength of atomic attraction among atoms within film and atoms in the films with substrate, three common growth modes are all observed for electrochemically deposited films. These modes are: Frank-van der Merwe (FM) growth, Stranski-Krastanov (SK) growth, and Volmer-Weber (VW) growth (Fig. 5a-c). Frank-van der Merwe growth happens when atoms of the film are preferentially attracted to the substrate, resulting in smooth two-dimensional (2D) layer-by-layer growth. Volmer-Webber growth takes place when atoms in the films are more strongly bonded compared to their bonding to the substrate. So threedimensional adatom islands are seen on the substrate. Stranski-Krastanov growth is an intermediary process of the first two growth modes.

Besides these three primary growth modes, electrochemical deposition also has an analogical mode to the atomic layer epitaxy for vapor phase deposition. It is called electrochemical atomic layer epitaxy (EC-ALE). Even though the resulting smooth film morphology is similar to that under FM growth, the intermediate deposition process is different. For FM growth, a 2D layer of material, for example, a layer of compound material AB is deposited onto the substrate. On the contrary, in EC-ALE, a layer of A atoms are first deposited on the substrate followed by a second layer of B atoms and these two atomic layer form a 2D layer of compound material, as shown in Fig. 5d. There exists also another growth mode called ion exchange epitaxy (Fig. 5e), which has the adjustability of nanocrystal identity and size similar to liquid-phases synthesis as well as epitaxy control similar to molecular beam epitaxy [17]. An interesting morphology of epitaxial polymer nanowire growth on substrate, shown in Fig. 5f was demonstrated by Yan's [18] and Sakaguchi's [19] group. Their experiments will be discussed in detail in the following context.

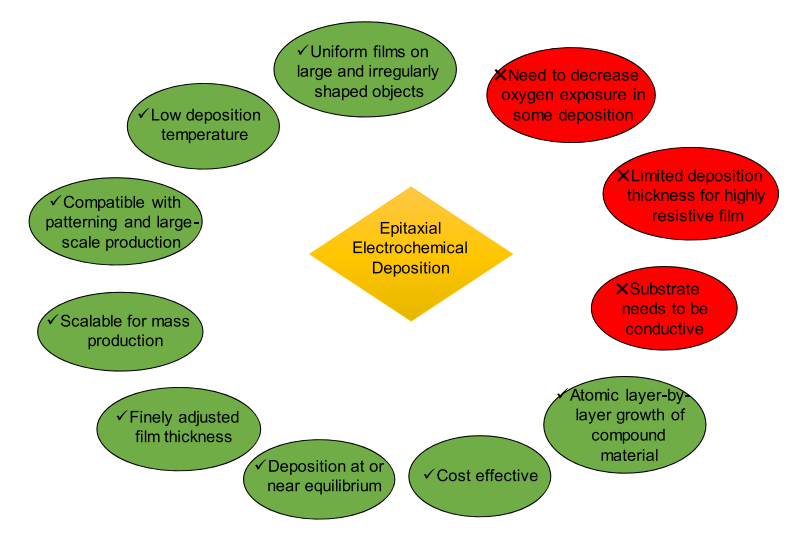


Fig. 2. Advantages and disadvantages of epitaxial electrochemical deposition.

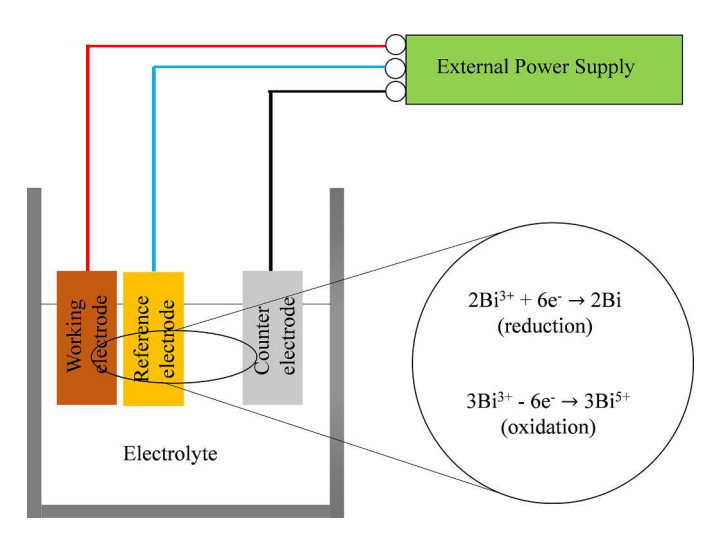


Fig. 3. A schematic sketch of the electrochemical deposition system.

In this review, we will present the ability of electrochemical deposition in synthesizing epitaxial nanostructures for a large category of materials, such as metals, element and compound semiconductors, oxides and organics. The review can serve as a reference when considering using electrochemical deposition in fabricating epitaxial materials.

## Electrochemical epitaxy of nanostructures

In this session, we discuss in details on materials belonging to different categories being successfully synthesized by epitaxial electrochemical deposition. The deposition systems, growth modes, material morphology and applications are studied.

## Metals

Metals, being conductive, can be easily deposited on electrode by electrochemical deposition to the desired thickness. However, in order for the deposited metal layer to be functional as the electrode component in electronic and magnetic devices, or as a catalyst layer, i.e. Pt layer, or as a buffer layer for further deposition of sequential materials,

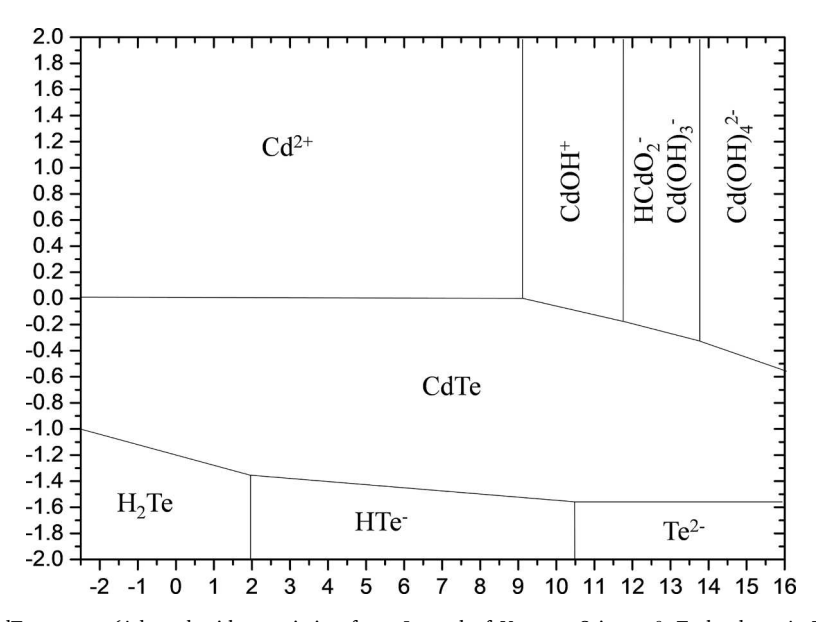


Fig. 4. Pourbaix Diagram for CdTe system. (Adapted with permission from Journal of Vacuum Science & Technology A: Vacuum, Surfaces, and Films, 10 (1992) 886–891.).

4

Nano Trends 4 (2023) 100024

(continued on next page)

 Table 1

 Summary of materials prepared by epitaxial electrodeposition.

Material	Approach	Electrolyte	Substrate	Temperature	Growth mechanism	Morphology	Applications	Refs.
Pt	Electrochemical	$K_2$ PtCl <sub>4</sub> —NaCl solution	Single crystalline Au (111)	N.A.	Underpotential deposited hydrogen is used to control and terminate Pt deposition	Monolayer of Pt	Catalyst	[24]
Pt	Surface-limited redox replacement reaction and electrochemical atomic layer epitaxy (EC-ALE)	$HClO_4/H_2SO_4$ — $CuSO_4$ - $PtCl_4^2$ solution	Au (111)	N.A.	Layer-by-layer growth	Atomically ordered Pt nanofilms on well defined Au (111)	Catalyst	[26]
Pt	Electrochemical	KAuCl <sub>4</sub> –for deposition of Au buffer layer K2PtCl4-NaCl-for deposition of Pt	3D Ni foam-based substrate with Ag or Au buffer layer	N.A.	Underpotential deposited hydrogen is used to control and terminate Pt deposition	Monolayer of Pt	Catalyst	[25]
Au	Electrochemical/Epitaxial lift-off	${\rm HAuCl_4\text{-}KCl\text{-}H_2SO_4\text{-}K_2SO_4} \ solution$	Hydrogen terminated Single- crystal Si(111) with a 0.2° miscut toward [112]	N.A.	Electrodeposition of single Au film on Si followed by epitaxial lift off of Au film	Single crystal Au foil	Buffer layer	[20]
Au	Electrochemical	$\label{eq:hauCl4-KCl-H2SO4-K2SO4} HAuCl_4\text{-KCl-H}_2\text{SO}_4\text{-K}_2\text{SO}_4 \text{ solution}$	Hydrogen terminated Single- crystal Si(111) with a 0.2° miscut toward [112]	N.A.		(111) orientated Au layer in strong epitaxy with the substrate	Buffer layer	[21]
Au	Electrochemical	KAu(CN) <sub>2</sub> —NaCN—NaOH solution	Hydrogen terminated Single- crystal Si(111) with a 0.2° miscut toward [112]	N.A.	3D island growth followed by layer-by- layer growth	Densely packed nm-sized Au islands homogeneously distributed on the H-Si(111) terraces. Their size increases with increasing gold coverage before a continuous Au film is formed across the entire sample surface.	Buffer layer	[22]
Ag	Surfactant Mediated Electrochemical	AgClO <sub>4</sub> -Pb(ClO <sub>4</sub> ) <sub>2</sub> —HClO <sub>4</sub> .	Au (111)	N.A.	Layer-by-layer			[31]
Ag	Electrochemical	$\mbox{HClO}_4\mbox{-AgClO}_4$ and a mediator of $\mbox{Pb}(\mbox{ClO}_4)_2$ or Cu $(\mbox{NO}_3)_2$ solution	Au (111)	N.A.	Stranski-Krastanov growth	Atomically flat, epitaxial, single- crystal thin films (~150 nm in thickness)		[27]
Ag	Repetitive Pb adlayer underpotential deposition (UPD) and stripping cycles during Ag bulk deposition.	Ag <sub>2</sub> SO <sub>4</sub> -PbO—HClO <sub>4</sub>	Au (111)	N.A.	Layer-by-layer growth	Two-dimensional growth of ultra-thin metal film		[30]
Ag	Irreversible galvanic displacement of underpotentially predeposited less-noble metal by a more-noble metal of interest.	For electrochemical deposition: Pb (ClO <sub>4</sub> ) <sub>2</sub> —NaClO <sub>4</sub> —HClO <sub>4</sub> For galvanic displacement: AgClO <sub>4</sub> —HClO <sub>4</sub>	Аи (111)	RT.	Frank–van der Merve or layer-by-layer 2D growth	quasi-perfect, twodimensional growth of up to 35 layers of Ag on Au (111)		[29]

Table 1 (continued)

5

Material	Approach	Electrolyte	Substrate	Temperature	Growth mechanism	Morphology	Applications	Refs.
Ag	Electrochemical (underpotential deposition and overpotential deposition)	1. Ag(ClO <sub>4</sub> )-Pb(ClO <sub>4</sub> ) <sub>2</sub> —NaClO <sub>4</sub> —HClO <sub>4</sub> 2. Pb(ClO <sub>4</sub> ) <sub>2</sub> -Tl(ClO <sub>4</sub> )-NaClO <sub>4</sub> —HClO <sub>4</sub> 3. Ag(ClO <sub>4</sub> )-Pb(ClO <sub>4</sub> ) <sub>2</sub> - Tl(ClO <sub>4</sub> )-NaClO <sub>4</sub> —HClO <sub>4</sub>	1. Au (111) 2. Ag (111) 3. Au (111)	N.A.	Layer-by-layer formation of Different heterostructured ultra- thin metal films	Heterostructured ultra-thin metal films		[28]
Bi	Electrochemical/ Annealing	$\mathrm{Bi(NO_3)_3\cdot5H_2O}$ solution	Si (100) wafer with a thin Au underlayer (~100 Å thick) pattern	N.A.	Polycrystalline Bi film is obtained after electrodeposition and annealing at 268 °C for 6 h in Ar results in single crystal Bi film	Single crystal Bi film with the trigonal axis orientated perpendicular to the substrate plane.	Magnetoresistance devices	[37]
Cu	Electrochemical	$\rm CuSO_4\!\!-\!\!H_2SO_4$	Au (111)	N.A.	Stranski-Krastanov growth	After formation of one monolayer Cu at underpotentials, 3D Cu clusters grow at surface defects		[36]
Cu	Electrochemical	$\rm CuSO_4-H_2SO_4$	Ag (111)	N.A.	Volmer-Weber growth	At low overpotentials: formation of Cu monoatomic high islands which are pseudomorphic on Ag. 2D growth of Cu deposit continues up to the second layer. At high overpotentials: nucleation of Cu at surface defects followed by three dimensional cluster growth.		[34]
Cu	Electrochemical	$\rm CuSO_4-H_2SO_4$	Ag (111)	N.A.		Cu electrodeposited on Ag(100) grows pseudomorphic up to the eighth layer. Very abruptly a new surface structure begins to emerge with the seposition of the ninth layer. This structure transformation causes the top layer to be buckled.		[35]
Cu	Defect-mediated electrochemical	Cu(NO <sub>3</sub> ) <sub>2</sub> —HClO <sub>4</sub> -Pb(ClO <sub>4</sub> ) <sub>2</sub>	Au (111)	N.A.	Layer-by-layer growth	top layer to be buckled.		[32]
Cu	Surface-limited redox replacement reaction and electrochemical atomic layer epitaxy (EC-ALE)	Electrodepositon: Pb(ClO <sub>4</sub> ) <sub>2</sub> —NaClO <sub>4</sub> —HClO <sub>4</sub> Redox replacement: Cu(ClO <sub>4</sub> ) <sub>2</sub> —HClO <sub>4</sub>	Au(111) or Ag (111)	N.A.	Layer-by-layer growth	Epitaxial Cu up to 100 monolayer on the substrate		[33]
Co	Electrochemical	Na <sub>2</sub> SO <sub>4</sub> —CoSO <sub>4</sub>	Cu (001)	N.A.			Thin film magnetism	[23]
Si	Electrocrystallization epitaxy	KF-LiF-K <sub>2</sub> SiF <sub>6</sub>	Si (111)	750 °C	v1.1	*** 1		[38]
Ge	Electrochemical liquid phase epitaxy	Thin liquid eutectic gallium indium films	Si	<i>T</i> ≤90 °C	Liquid-phase epitaxy	High crystalline quality Ge epifilms		[40]
	phase epitaky					ос сришно	(continued on	next nage)

Table 1 (continued)

Material	Approach	Electrolyte	Substrate	Temperature	Growth mechanism	Morphology	Applications	Refs.
Те	Electrochemical Atomic Layer Epitaxy (ECALE)	${ m TeO_2-H_2SO_4}$	Au (111)	N.A.	Layer-by-layer growth	Commensurate with the formation of higher coverage structures of Te, a roughening transition takes place, where the surface becomes pitted, resulting in about 40 % of the surface being covered with single atom deep pits.		[39]
Fe <sub>83</sub> Ga <sub>17</sub>	Electrochemical	Na3 –citrate-FeSO4-Ga2 (SO4)3 (mixed in the same order) with p H adjusted to 3.75 using dilute NaOH	1. n-GaAs (001) 2. polycrystalline brass	N.A.		1. Films are highly textured with $\langle 001 \rangle$ orientation along the substrate normal 2. films exhibit $\langle 011 \rangle$ preferred orientation	Spintronics applications	[68]
CuI, CdS	Electrochemical /Chemical	Solution containing metal ion and then solution containing $I^-$ or $\mathbf{S}^{2-}$	Graphite	N.A.	Solution phase method for growing supported quantum dots	Quantum dots with adjustable nanocrystal identity, diameter and excellent size monodispersity deposited on graphite with a defined orientation and electrical contact to the outside world		[17]
CdTe	Electrochemical Atomic Layer Epitaxy (ECALE)	$ m H_2SO_4 ext{-}TeO_2 ext{-}CdSO_4$	1. Au (100) 2. Au (100) Au (110) Au(111)	RT.	One element be deposited by reductive UPD while the other is deposited by oxidative UPD. (Layer- by-layer)	Bilayer of CdTe	Optoelectronic devices	1. [16] 2. [41]
CdSe	Electrochemical Atomic Layer Epitaxy (ECALE)	H <sub>2</sub> SO <sub>4</sub> -SeO <sub>2</sub> —CdSO <sub>4</sub> solution	Au (111) Au (110) Au (100)	N.A.	Layer-by-layer growth			[43]
CdS	Electrochemical Atomic Layer Epitaxy (ECALE)	For S atomic layer: Na <sub>2</sub> S-Na <sub>4</sub> P <sub>2</sub> O <sub>7</sub> —NaOH; For Cd atomic layer: CdSO4-Na4P2O7-NaOH	Ag (111)	N.A.	Layer-by-layer	Extremely small thickness a few Angstroms of CdS was deposited in Ag substrate	Nanometric material used in technological applications	[45]
CdS	Confined electrochemical Atomic Layer Epitaxy (ECALE)	3CdSO <sub>4</sub> ·8H <sub>2</sub> O─Na <sub>2</sub> S-HClO <sub>4</sub> −NH <sub>3</sub>	Ag (111) with patterned self- assembled monolayers (SAMs) of alkanethiolates	N.A.	Layer-by-layer	Ordered array of nanoclusters of CdS	sensors, photovoltaic, photoelectrochemical cells and more generally nanoscience	[46]
CdSe	Electrochemical Atomic Layer Epitaxy (ECALE)	For Se atomic layer: H <sub>2</sub> SO <sub>4</sub> —Na <sub>2</sub> B <sub>4</sub> O <sub>7</sub> -SeO <sub>2;</sub> For Cd atomic layer: CdSO <sub>4</sub> —CH <sub>3</sub> COOH—CH <sub>3</sub> COONa-Na <sub>2</sub> SO <sub>4</sub>	Au (111)	RT.	Layer-by-layer	Monolayer of CdSe on Au		[44]
CdTe, CdSe, CdS	Electrochemical Atomic Layer Epitaxy (ECALE)	For CdTe: Na <sub>2</sub> SO <sub>4</sub> —HTeO <sub>2</sub> <sup>+</sup> and CdSO <sub>4</sub> -acetate For CdSe: NaClO <sub>4</sub> —HSeO <sub>3</sub> <sup>-</sup> and CdSO <sub>4</sub> -acetate For CdS: NaClO <sub>4</sub> —Na <sub>2</sub> S·9H <sub>2</sub> O—NaOH and CdSO <sub>4</sub> -acetate	Si (100) coated with Ti and Au	N.A.	Layer-by-layer growth	Films formed with 200 or less cycles generally show a smooth morphology; however, deposits made with 500 or more cycles show increased amount of particles or crystallites.		[42]

Nano Trends 4 (2023) 100024

Table 1 (continued)

Material	Approach	Electrolyte	Substrate	Temperature	Growth mechanism	Morphology	Applications	Refs.
ZnSe	Electrochemical Atomic Layer Epitaxy (ECALE)	For Se atomic layer deposition: Na <sub>2</sub> SeO <sub>3</sub> ·5H <sub>2</sub> O—HClO <sub>4</sub> —NH <sub>3</sub> For Zn atomic layer deposition: ZnSO <sub>4</sub>	Ag (111)	N.A.	Layer-by-layer growth		optoelectronic devices	[47]
HgSe	Electrochemical Atomic Layer Epitaxy (ECALE)	HgO/SeO <sub>2</sub> —Na <sub>2</sub> SO <sub>4</sub> —H <sub>2</sub> SO <sub>4</sub>	300 nm thick gold film on glass	N.A.	Layer-by-layer growth	Deposited film possesses zinc blende structure, with a strong (111) preferred orientation.	Optoelectronics	[49]
HgSe	Electrochemical Atomic Layer Epitaxy (ECALE)	${\rm HgCl_2}$ complexed with ethylenediamine tetraacetic acid (EDTA)/HSeO $_3^ {\rm H_2SO_4-Na_2SO_4}$	Glass microscope slides with a 3 nm Ti adhesion layer and 600 nm of Au. Substrates	N.A.	Layer-by-layer growth	HgSe deposits were polycrystalline, with a strongly preferential (111) orientation.	Optoelectronics	[50]
$\rm In_2Se_3$	Electrochemical Atomic Layer Epitaxy (ECALE)	For In atomic layer deposition: In <sub>2</sub> (SO4) <sub>3</sub> —CH <sub>3</sub> COONa·3H <sub>2</sub> O—H <sub>2</sub> SO <sub>4</sub> —NaClO <sub>4</sub> For Se atomic layer deposition: SeO <sub>2</sub> —CH <sub>3</sub> COONa·3H <sub>2</sub> O—H <sub>2</sub> SO <sub>4</sub> —NaClO <sub>4</sub>	Glass microscope slides coated first with Ti, then with Au	RT.	Layer-by-layer growth	The thin film consists of particles that are between 70 and 200 nm in diameter, which are conformal with the Au substrate.	photovoltaic and photoelectrochemical devices	[48]
PbSe	Electrochemical Atomic Layer Epitaxy (ECALE)	Pb(ClO <sub>4</sub> ) <sub>2</sub> / SeO <sub>2</sub> —CH <sub>3</sub> COONa·3H <sub>2</sub> O—CH <sub>3</sub> COOH—NaClO <sub>4</sub>	Glass microscope slides coated first with Ti, and then with Au	N.A.	Layer-by-layer growth	Deposited film possesses rock salt structure for PbSe with a preferred (200) orientation.	Photodetectors, photoresistors and photoemitters in the infrared	[51]
$Bi_2S_3$	Electrochemical Atomic Layer Epitaxy (ECALE)	For S atomic layer: Na <sub>2</sub> S-CH <sub>3</sub> COONa-KOH; For Bi atomic layer: Bi(NO <sub>3</sub> ) <sub>3</sub> —HNO <sub>3</sub>	Au (111)	N.A.	Layer-by-layer	Well-ordered Bi <sub>2</sub> S <sub>3</sub> film deposited on Au substrate	Optoelectronic devices	[54]
$\mathrm{Bi}_{2}\mathrm{Te}_{3}$	Electrochemical Atomic Layer Epitaxy (ECALE)	Bi(NO3)3·5H2O/TeO <sub>2</sub> —HClO <sub>4</sub>	Pt coated Si (100)	RT.	Layer-by-layer	Smooth film with monodispersed feature sizes	Thermoelectric devices	[52]
γ-CuI	Electrochemical reaction- chemical	Cu(II)-EDTA-KI solution	Au (100)	50 °C		Epitaxial film of CuI (111) on Au (100)	Electrolyte for high hole mobility in dye-sensitized solar cell; catalyst in organic synthesis; application in the formation of both inorganic and biochemical supramolecular compounds	[11]
γ-CuI	Electrochemical reaction- chemical	Cu(II)-EDTA-KI solution	Indium doped tin oxide (ITO)	RT.		CuI film with preferential orientation along (111) crystal axis	Electrolyte for high hole mobility in dye-sensitized solar cell; catalyst in organic synthesis; application in the formation of both inorganic and biochemical supramolecular compounds	[53]
I-Ag superlattice	Electrochemical	AgClO <sub>4</sub> —HClO <sub>4</sub> solution	Iodine pretreated Pt (111)	N.A.		Iodine layer remains attached to the Pt surface and ordered Ag layers are	•	1. [69] 2.

Material	Approach	Electrolyte	Substrate	Temperature	Growth mechanism	Morphology	Applications	Refs.
PbSe/PbTe Superlattice	Electrochemical Atomic Layer Epitaxy (ECALE)	Pb(ClO <sub>4</sub> ) <sub>2</sub> —CH <sub>3</sub> COONa·3H <sub>2</sub> O-TeO <sub>2</sub> -SeO <sub>2</sub> - KOH—NaClO <sub>4</sub>	Glass microscope slides coated first with Ti, and then with Au	N.A.	Layer-by-layer growth	Superlattice of PbSe/PbTe are formed with a small amount of 3D growth due to excessive deposition conditions	Thermoelectric applications and infrared sensors	[71]
Yttrium-stabilised Zirconia (YSZ)	Electrochemical	YSZ solid electrolyte	Ni particles in porous Ni/yttria- stabilised zirconia (Ni/YSZ) system	1073 K or 1123 K	Volmer-Weber growth	Well bonded YSZ nanoparticles with cubic symmetry (tetragonal symmetry may also exist) on Ni grains	Heterogeneous joining at the micro-/nanoscale	[64]
$Ba_{1-x}K_xBiO_{3+y}$ (0.32 $\le x \le 0.53$ )	Electrochemical	KOH-Bi <sub>2</sub> O <sub>3</sub> -BaO—H <sub>2</sub> O melt	(100) <sub>c</sub> orientated BaBiO <sub>3</sub> and Ba <sub>0.8</sub> K <sub>0.2</sub> BiO <sub>3</sub>	240 °C		C		[58]
Fe <sub>3</sub> O <sub>4</sub>	Electrochemical	K(CH3COO)-Fe(NH4)2(SO4)2·6H2O	Au (111)	90 °C			Magnetoelectronic devices	[59]
Fe <sub>3</sub> O <sub>4</sub>	Electrochemical	K(CH3COO)-Fe(NH4)2(SO4)2-6H2O	Au (110), (100), (111)	90 °C			Magnetoelectronic devices	[60]
Cu <sub>2</sub> O	Electrochemical	NaOH—Cu (II) sulfate pentahydrate-lactic acid solution	Au (100)	30 °C		High quality, epitaxial film of Cu <sub>2</sub> O grown on Au substrate	Study of negative differential resistance for Cu <sub>2</sub> O/Cu nanostructure	[62]
Cu <sub>2</sub> O	Electrochemical	CuSO <sub>4</sub> -lactic acid at pH=9.0 or 12.0	InP (001)	65 °C at pH=9.0; 25 °C at pH=12.0	Volmer-Weber growth	Pyramidal morphology of $\text{Cu}_2\text{O}$ islands grown at a pH of 9.0; Cubelike morphology of $\text{Cu}_2\text{O}$ islands grown at a pH of 12.0 with flat facets.	Study Bose–Einstein condensation in Cu <sub>2</sub> O material	[61]
Cubic polymorph of $Bi_2O_3$ ( $\delta$ - $Bi_2O_3$ )	Electrochemical	$\mathrm{Bi}(\mathrm{NO}_3)_3\text{-tartaric}$ acid-KOH solution	Au (110), (100), (111)	65 °C	Film has strong in-plane and out-of-plane orientation	Epitaxial single crystals of cubic $\mathrm{Bi}_2\mathrm{O}_3$ with high structural perfection	Fuel cells, oxygen sensors, and oxygen pumps	[63]
Poly (3- hexylthiophene) (P3HT)	Electropolymerization	Acetonitrile- $Bu_4NPF_6 \ solution$	Tin oxide (ITO) electrode modified by a highly oriented isotactic polypropylene (i- PP) ultrathin film	N.A.		Side-on orientation of P3HT molecules	Active layer in optoelectronic devices	[18]
Single- polythiophene wires	Electrochemical epitaxial polymerization	3-butoxy-4-methylthiophene (BuOMT), $NBu_4PF_6,\ dichloromethane\ (DCM),\ iodine$	Au (111)	N.A.	Step-by-step propagation of single conjugated-polymer wires along the lattice of an electrode surface.	Uniform high density array of single conjugated- polymer wires as long as 75 nm	High-performance molecular- and conjugated-polymer devices, such as field- effect transistors, light- emitting diodes and solar batteries	[19]

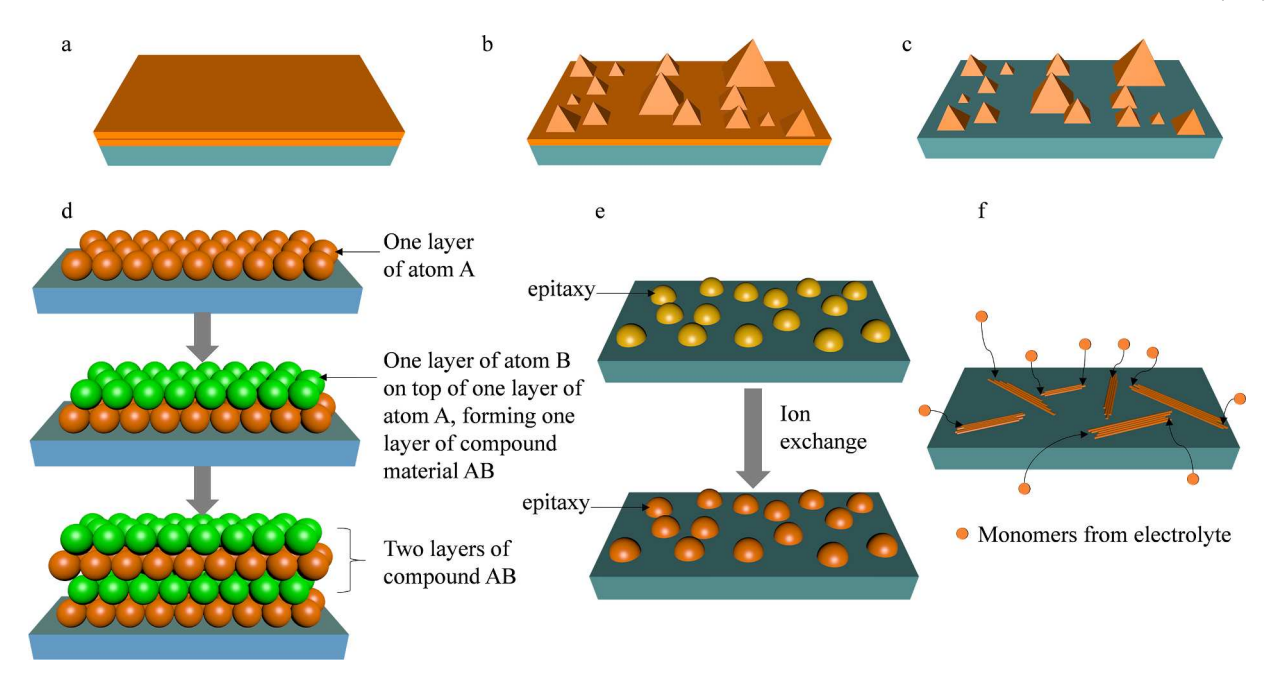


Fig. 5. Growth modes in epitaxial electrochemical deposition: (a) Frank-van der Merve growth; (b) Stranski-Krastanov growth; (c) Volmer-Weber growth; (d) Electrochemical atomic layer epitaxy; (e) Ion exchange epitaxy. (f) epitaxial growth of nanowires on substrate.

uniform metal layers are desired. In technologies like molecular beam epitaxy, chemical/physical vapor deposition, pulsed-laser epitaxy, they can control the film morphology by controlling the substrate temperature. Thus, usually high growth temperature is needed in order for deposited metal atoms to have enough mobility to diffuse and rearrange themselves to low energy sites on the substrate. This high operation temperature not only introduces higher demands on system design and vacuum level but also may blur the heterogeneous boundary of the deposited metal layer with other layer component, degrading the interface quality. Due to its low temperature processing condition, electrochemical depositions of epitaxial metal films and nanostructures are investigated by many groups and show promising results.

Recently, Mahenderkar et al. [20] demonstrated epitaxial lift-off of wafer size single-crystal gold foils which was grown by electrochemical deposition. In this way, they successfully obtained the free-standing single-crystal gold film. In their experiment, they first grew epitaxial Au (111) on Si (111) substrate at room temperature by electrochemical deposition. A sacrificial  $\mathrm{SiO}_{x}$  layer was then introduced between Au film and Si substrate by photoelectrochemically oxidizing the original Si layer just below the Au film. A polymer adhesive was then applied on top of the Au film, followed by HF solution etching of the  $\mathrm{SiO}_{x}$  layer to finally separate the Au film from Si substrate. As shown in Fig. 6a, a Au single crystal film with 50.8 mm in diameter and 28 nm in thickness was obtained. High-resolution TEM cross-section images of as deposited Au

on Si (Fig. 6b) and pole figure (Fig. 6c) confirmed the epitaxy growth of Au (111) on Si (111). The report provides an inexpensive way to fabricate large metallic single crystal film which can serve as a high quality electrode in flexible optical and electronic devices.

Epitaxial electrochemical deposition of gold on hydrogen-terminated Si (111) substrate have been investigated by Prod'homme et al. [21] and Warren et al. [22]. In their studies, they tried to grow a high quality epitaxial Au as a buffer layer on Si for further deposition of magnetic ultra-thin films which possess interesting perpendicular magnetic anisotropy (PMA), possible for high density data storage devices. The growth mode for epitaxial Au layer deposition was found to be either 3D island growth (at pH=14) or 2D layer-by-layer growth (at pH=4), clearly controlled by the pH value of electrolyte. Besides gold, copper also serves as a good buffer layer for further deposition of ultra-thin magnetic materials. In 1997, Schindler and Kirschner deposited ultra-thin epitaxial Co film on Cu (001) substrate by electrochemistry [23]. They were able to finely adjust the magnetic film thickness in monolayer range and there were no magnetically dead layers in the deposited film.

Another noble metal, Pt, an important catalyst was synthesized in epitaxial film form by electrocheimcal deposition [24–26]. Among them, Liu et al. [24] employed self-terminating electrodeposition at room temperature to grow two-dimensional monolayer Pt film on Au (111) surface with underpotential deposited H ( $H_{upd}$ ). Fig. 7 shows a

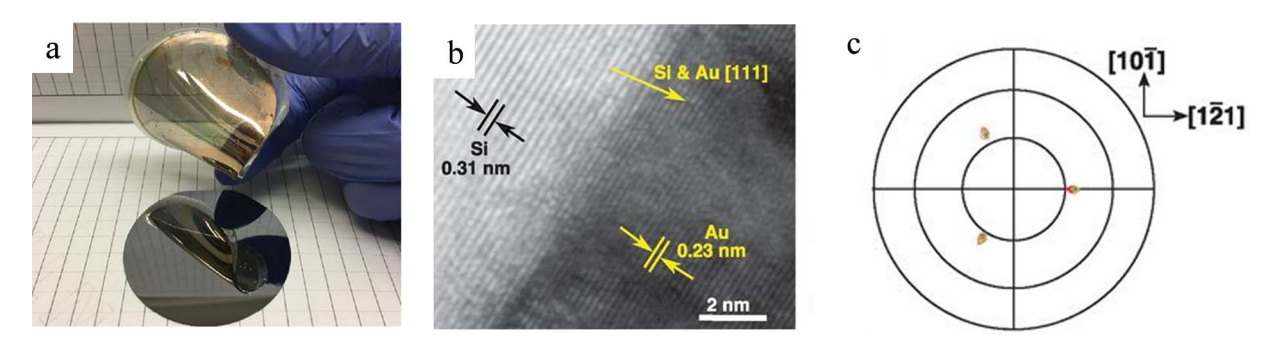


Fig. 6. (a) Wafer-size Au foil. (b) High-resolution TEM image of as deposited Au epitaxial film on Si substrate. (c) (220) pole figure of Au(111) foil. (Adapted with permission from Science, 355 (2017) 1203–1206.).

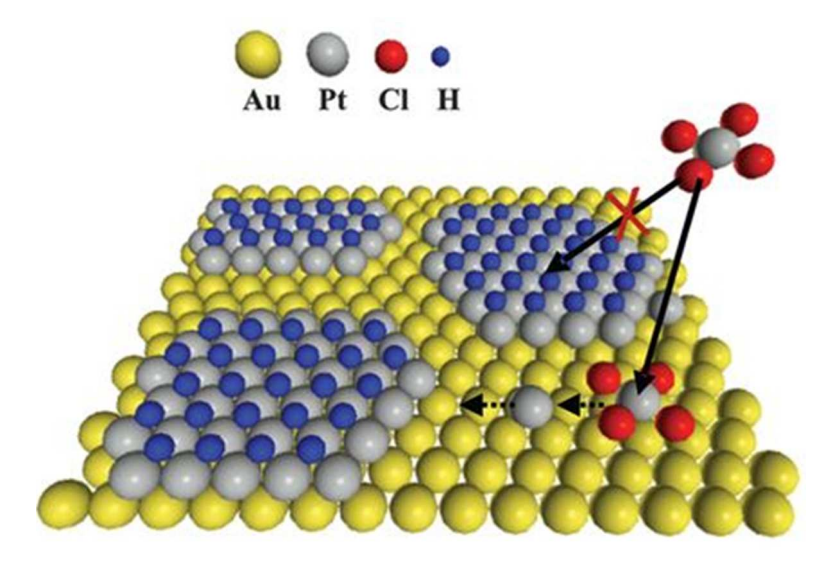


Fig. 7. A schematic of Pt deposition on Au (111). (Adapted with permission from Science, 338 (2012) 1327–1330.).

schematic demonstration of the 2D growth of Pt film on Au substrate terminated by  $H_{\rm upd}$ . The  $H_{\rm upd}$  helps to hinder the development of a second Pt layer while expanding the 2D Pt islands. Further growth of thicker Pt films to desired thickness can be achieved by removing the  $H_{\rm upd}$  layer by sweeping the potential into more positive values. The ability to prepare thin Pt films can reduce the Pt loading in catalysts while maintaining the catalyst performance.

Epitaxial electrochemical deposition of Ag on Au substrate by introducing Pb or Cu adlayers were explored by some groups [27–31]. Their studies demonstrated a defect, or surfactant mediated strategy to realize the continuous 2D epitaxial thin film growth instead of thermodynamically 3D island growth under ambient temperature. Such strategy may also be applied in other deposition systems. For example, epitaxial copper film has also been electrochemically deposited on Au substrate via defect-mediated growth [32]. Viyannalage et al. also employed a surface limited redox replacement strategy to grow copper on Ag and Au substrates [33]. Kolb's group conducted a detailed study on the initial stages of Cu electrodeposition on Ag (100), Ag (111) and Au (111) substrates by *in-situ* scanning tunneling microscopy to investigate the initial nucleation and growth process of Cu films [34–36].

Yang, etc., [37] synthesized single crystal Bi film of 1–20 micrometer by electrochemical deposition and annealing. Polycrystalline Bi film was obtained after electrochemical deposition using thin Au ( $\sim$ 100 Å thick)

patterned Si (100) wafer. Subsequent annealing at 268 °C for 6 h in Ar atmosphere converted the polycrystalline Bi film to single crystal. The XRD and pole-figure scan of (116) peaks (Fig. 8a and b) confirmed the high crystallinity of the prepared Bi film. Due to high quality of the single crystal Bi film, large magnetoresistance (MR) was measured, contributed by long effective mean free path for carriers. Its MR effect was orders of magnitude larger than Bi film with small grains prepared by evaporation or sputtering. Fig. 8c-f display the quasi-linear curve of MR with respect to magnetic field H in different measuring geometries under 5 K and 300 K for both as-deposited polycrystalline and annealed single crystalline Bi film. The large room temperature MR (200-300 %) given various magnetic field orientations is of interest for technological applications. The non-hysteresis and quasi-linear MR vs. H relation shows potential applications in wide-range field and current sensors and the device sensitivity is not expected to loss while measuring fields in different directions with respect to the device.

Metals, renowned for their electrical conductivity, can be electrochemically deposited with high precision through electrochemical deposition at lower temperatures, making them ideal for use in electronic, magnetic, and catalytic devices.

Epitaxial electrochemical deposition enables the growth of singlecrystal metal foils, like gold on silicon substrates, useful in flexible optical and electronic devices. Single-crystal bismuth films, synthesized by

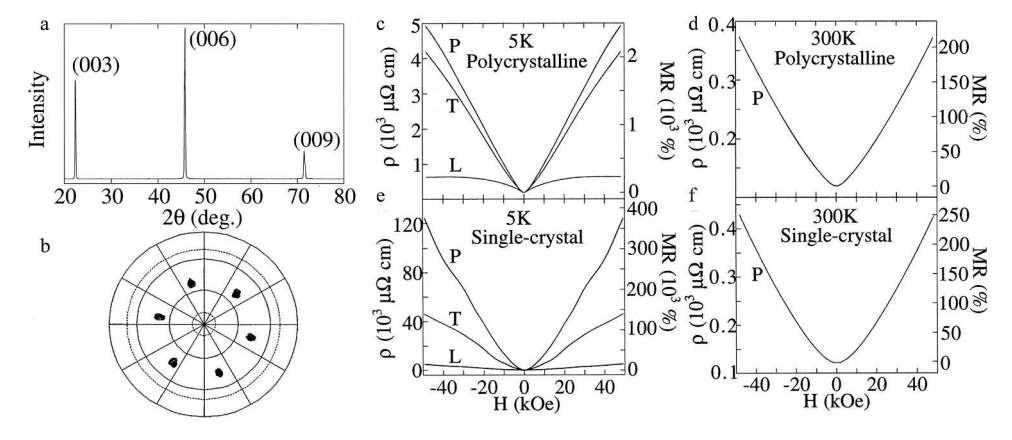


**Fig. 8.** (a) X-ray diffraction patterns of a 5-μm-thick single-crystal Bi film. (b) Pole-figure scan of the (116) peaks exhibiting six-fold symmetry. (c-f) The MR of a 20-μm-thick electrodeposited Bi film: (c) as-deposited polycrystalline film at 5 K in the perpendicular (P), transverse (T), and longitudinal (L) geometries; (d) as-deposited film at 300 K in the P geometry; (e) single-crystal film at 5 K in the P, T, and L geometries; and (f) single-crystal film at 300 K in the P geometry. (Adapted with permission from Science, 284 (1999) 1335–1337.).

electrochemical deposition demonstrate exceptional crystallinity and magnetoresistance, promising for sensors and electronics. In magnetic materials, it creates buffer layers, such as gold and copper, crucial for ultra-thin magnetic film deposition, suitable for high-density data storage. For catalysis, it simplifies the growth of thin platinum films, reducing the need for precious metals, benefiting fuel cells and catalytic processes. Moreover, defect-mediated strategies in electrochemical deposition have opened doors to continuous 2D epitaxial thin film growth. Epitaxial electrochemical deposition offers greater control and versatility in materials fabrication. It addresses the need for uniform metal layers, crucial for optimal device performance.

#### Semiconductors

Semiconductors build up the foundation of current technology. They play important roles in electronic, magnetic and optical devices, as well as in investigation on fundamental science. Semiconductor devices generally contain several layers and it is crucial to have sharp, high quality interface to enhance device performance and stability. Electrochemical deposition, with its unique capability of obtaining epitaxial thin films at low temperatures, shows promising applications in fabrication of sharp heterojunctions due to limited thermal diffusion. Low-temperature synthesis is also beneficial for reducing thermal stresses, enhancing material capability and saving energy [38]. In this session, electrochemical deposition of both element semiconductors and compound semiconductors are discussed.

#### (a) Element semiconductors

In 1976, U. Cohen and Robert A. Huggins realized epitaxial Si (111) film growth on Si (111) substrate serving as a cathode with another high purity Si serving as dissolving anode in molten fluorides system [38]. The deposition is conducted at 750  $^{\circ}\text{C}$ , relatively low compared to the temperature used in CVD process. The stable fluoride ion complexes were believed to decrease diffusion-controlled effects, achieving uniform epitaxial film growth at low temperatures. Fig. 9 shows the scanning electron micrograph of epitaxial Si layer deposited at constant current of 4 mA/cm².

Sorenson et al. demonstrated successful synthesis of chalcogenide atomic layer, Te, on Au (111) substrate from aqueous solution by under potential deposition (UPD) [39]. Initial nucleation and growth of Te films were studied by in-situ scanning tunneling microscopy, low energy electron diffraction and Auger electron spectroscopy. Higher coverage film structures finally led to a roughening transition and pitted surface was observed. This study on chalcogenide thin film growth is important



**Fig. 9.** SEM photographs of (111) Si epitaxy layers grown at 4 mA/cm2. (Adapted with permission from J. Electrochem. Soc., 123 (1976) 381–383.).

in surface chemistry and in further growth of II-VI compound semi-conductor devices.

Very recently, Demuth et al. [40] successfully deposited another element semiconductor, epitaxial Ge thin films, on single crystal Si wafer despite their large lattice mismatch (~4.2 %). They demonstrated the growth of epitaxial Ge on Si for the first time by electrochemical liquid-phase epitaxy involving liquid eutectic GaIn thin film serving as both electrode and solvent. The deposition was conducted at ambient pressure and temperatures below the melting temperature of water. Fig. 10a shows a cross-section image of Ge-Si (111) interface by high-resolution TEM. It displays a continuous Ge film across the interface without apparent voids. Selective area electron diffraction patterns (Fig. 10b and c) collected from pure Ge film and Ge/Si interface showed same crystalline orientation, indicating a good epitaxial relation with the substrate. Fig. 10d is the pole figure generated from electron back scatter diffraction of Ge film on Si (100) substrate, and they demonstrated good registry between film and both underlying substrate and surrounding film. This work demonstrated the powerful simple and tunable electrochemical liquid-phase epitaxy method in electrodepositing any material with a liquid metal carrying proper electrochemical and metallurgical properties. These heterojunctions composed of highly crystalline films have wide applications in optoelectronic technologies.

## (a) Compound semiconductors

Epitaxial chalcogenide films, CdTe [16,41,42], CdSe [42–44], CdS [17,42,45,46], ZnSe [47],  $In_2Se_3$  [48], HgSe [49,50], PbSe [51],  $Bi_2Te_3$  [52] and  $Bi_2S_3$  [53], as well as epitaxial halides films, CuI [11,17,54] have been successfully synthesized by electrochemical deposition.

One deposition method is electrochemical atomic layer epitaxy (ECALE) demonstrated by Gregory and Stickney's group [16]. It deposits materials one atomic layer by one atomic layer which is proved to be very useful in synthesizing such thin film compound semiconductors with good crystallinity and strong orientation preference with respect to the substrates. The film thickness can be controlled by the number of EC-ALE cycles.

In 1998, Colletti et al. [42] successfully synthesized a series of Cd-based chalcogenide thin films of CdTe, CdSe, and CdS on Si (100) coated with Ti and Au by EC-ALE. EC-ALE can separately deposit the two kinds of component atoms onto substrate to form epitaxial layers. The Cd source was proved by CdSO<sub>4</sub> and Te, Se, S sources were provided by HTeO<sub>2</sub><sup>+</sup>, HSeO<sub>3</sub><sup>-</sup> and Na<sub>2</sub>S·9H<sub>2</sub>O dissolved in electrolyte solutions, respectively. They obtained films had (111) preferred orientation with high signal of (111) peak to noise ratio, especially for CdTe and CdSe films. EC-ALE growth mode demonstrates its ability to prepare compound semiconductors with good crystallinity, stoichiometry and more freedom to control film thickness. EC-ALE can also be applied to deposit thin films on pre-patterned substrate. Cavallini et al. [46] deposited two-dimentional CdS film onto patterned self-assembled monolayers (SAMs) of alkanethiolates on Ag (111) substrate. CdS growth was confined to SAMs-free area of the substrate. Fig.11 shows a  $10 \times 10 \,\mu\text{m}^2$ morphology of CdS thin film after 20 cycles of EC-ALE growth. The images display self-organized well-aligned CdS nanostripes.

The disadvantage of ECALE method is the process is relatively complicated as electrolyte needs to be changed for each layer of deposition of compound material. A thin-layer electrochemical (TLE) cell configuration is developed to speed up the change of electrolyte solutions during deposition [55].

In another method, a single electrolyte is used during deposition. Selecting the proper single electrolyte may be challenging as need to take interactions among the various precursor species and interactions between electrolyte and substrate into consideration, but it also offers a faster deposition process as it does not need to change electrolyte throughout the deposition. Penner [17] employed electrochemical/chemical (E/C) method to synthesize CuI and CdS quantum

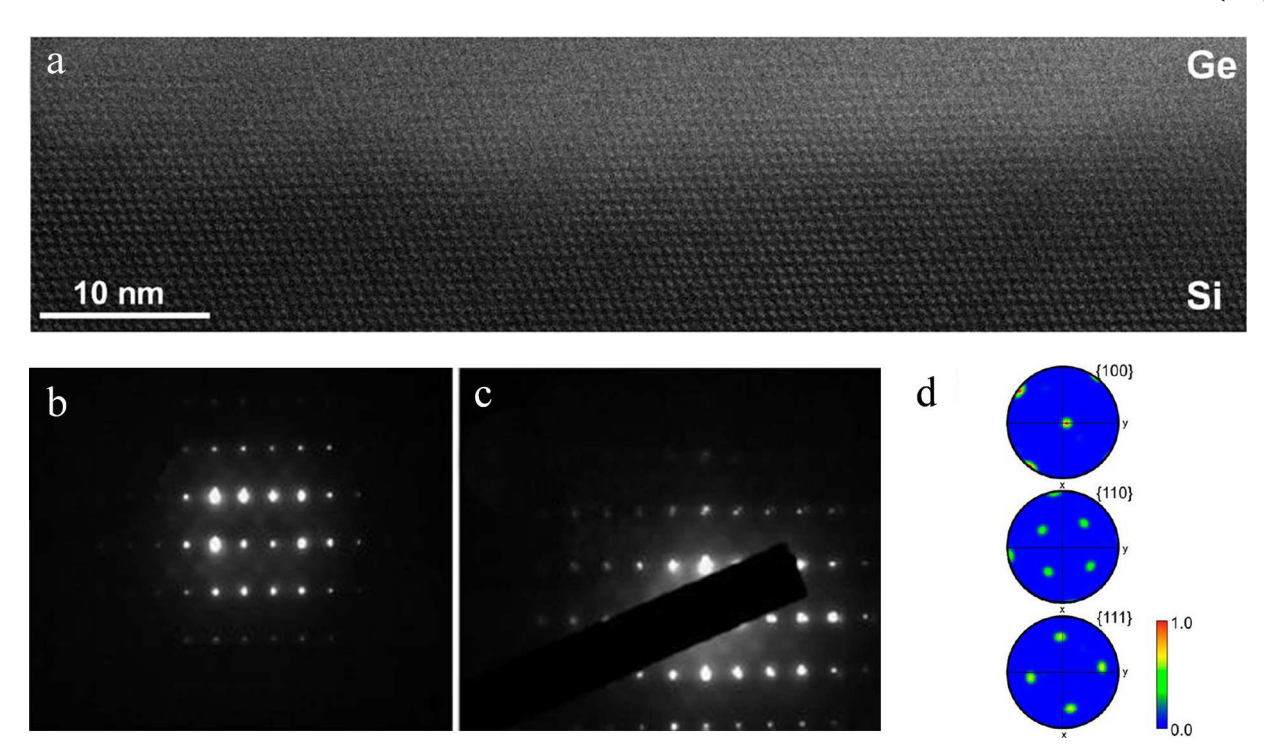


Fig. 10. (a) High resolution annular dark-field scanning transmission electron micrograph of the interface between the Ge film and Si substrate; (b,c) Electron diffraction patterns for the Ge film and the Ge/Si interface, respectively; (d) Contour pole figures from the EBSD mapping shown along the 110 and 111 poles. (Adapted with permission from Journal of the American Chemical Society, 139 (2017) 6960–6968.).

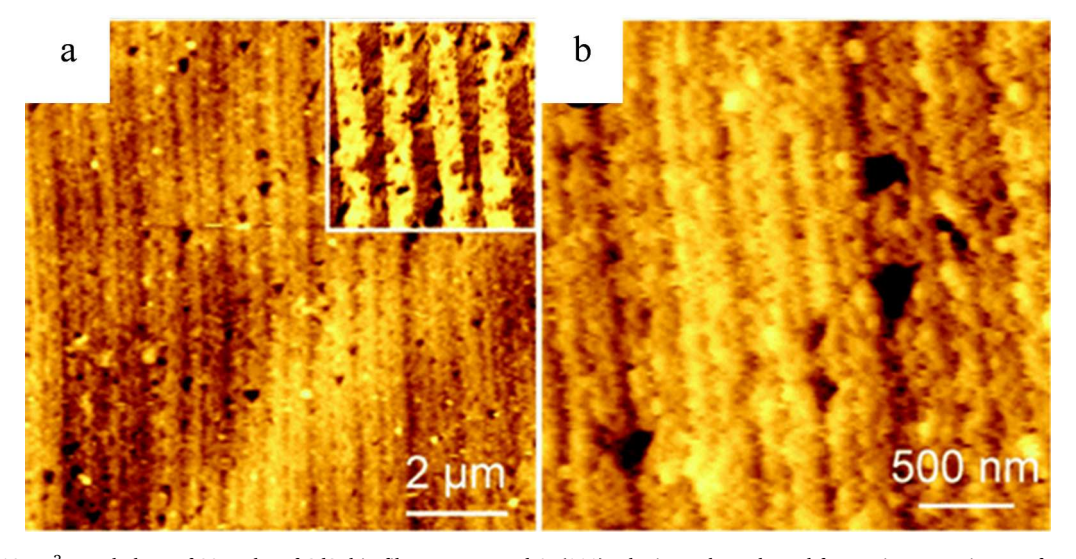
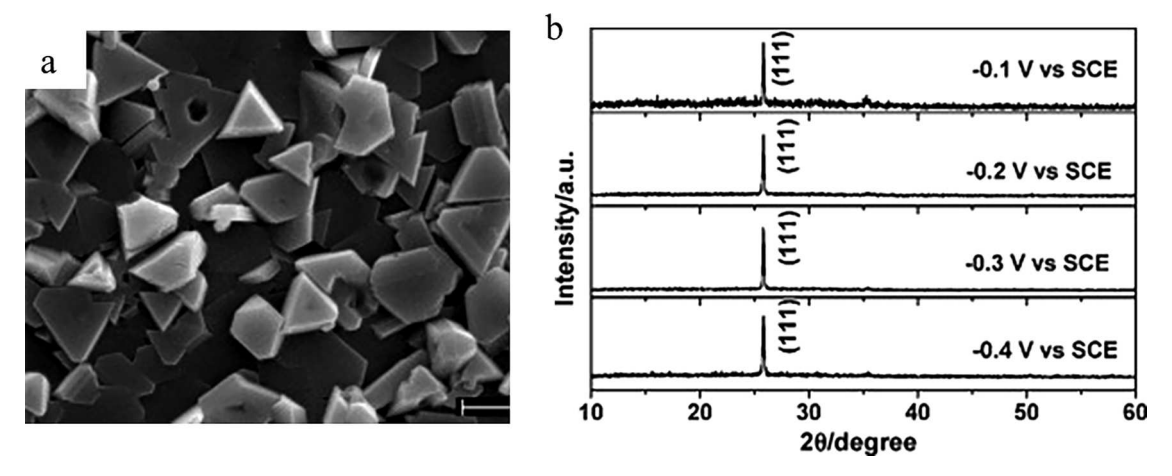


Fig. 11. (a)  $10 \times 10 \mu m^2$  morphology of 20 cycles of CdS thin film on patterned Ag(111). The inset shows lateral force microscopy image of patterned surface. (b) Detail of a. between the printed  $\mu$ -stripes of hexadecanethiol, the CdS clusters self-organize along parallel nanostripes. (Adapted with permission from The Journal of Physical Chemistry C, 111 (2007) 1061–1064.).

dots on graphite surface on a particle-by-particle basis. These quantum dots have adjustable nanocrystal identity, small size dispersity as well as preferred orientation on the substrate. The growth mode is shown in Fig. 5e, and an AFM image of CdS nanocrystals with mean core diameter of 75 Å on graphite is shown in Fig. 12a. Metal crystals, i.e. Cu, Cd, with similar size were first electrodeposited on graphite surface followed by electrochemical oxidation of metal particles to metal oxides and  $\rm O_2$  displacement of oxide ion by  $\rm I^-$  or  $\rm S^{2-}$ . The epitaxial deposition of CdS on graphite was proved by their diffraction pattern as shown in Fig. 12b, although how these nanocrystals locate the minimum energy site on the substrate surface without lateral motion remains unclear. This work provides a unique synthetic method to prepare nanocrystals with

attributes from both liquid-phases synthesis and molecular beam epitaxy. This E/C method was also employed by Mu [11], to prepare epitaxial  $\gamma$ -CuI onto Au (100) and indium doped tin oxide (ITO) substrate, respectively, from Cu(II)-ethylene diamine tetra-acetic acid disodium (EDTA) complex-KI electrolyte. The  $\gamma$  phase CuI possesses an ordered, face-centered cubic zinc blend structure. It is a p-type semiconductor with a wide band gap of 3.1 eV, which can be used as an electrolyte with high hole mobility in dye-sensitized solid-state solar cells. The Cu(II) was first reduced in EDTA solution by electrochemical process: Cu $^{2+}(aq)+e^{-}\rightarrow Cu^{+}(aq)$ . Then the Cu(I) ion combined with  $I^{-}$  ion in the electrolyte to form CuI through chemical reaction: Cu $^{+}(aq)+I^{-}(aq)\rightarrow CuI(s)$ . Fig. 13a shows SEM images of epitaxy  $\gamma$ -CuI film grown

Fig. 12. (a) Noncontact atomic force microscope (nanocrystal-AFM) images of graphite surfaces following the electrochemical/chemical synthesis of sulfur-capped CdS nanocrystals; (b) Selected area electron diffraction patterns (SAED) for CdS. Besides, a hexagonal array of diffraction spots from graphite is also shown in the pattern. (Adapted with permission from Acc. Chem. Res., 33 (2000) 78–76.).



**Fig. 13.** (a) SEM images of the γ-CuI film deposited on ITO substrate. (b) X-ray diffraction scan of γ-CuI on ITO substrate under different deposition potentials. (Adapted with permission from Electrochim. Acta, 55 (2010) 8121–8125.).

on ITO substrate respectively. X-ray diffraction characterizations (Fig. 13b) were conducted to reveal the crystal structures. It is worth noting that electrolyte normally used to introduce chalcogenides or halides elements usually have a low solubility in aqueous solution, and thus limiting the deposition rate by the transport of these elements to electrode [56]. When using a single electrolyte for deposition, an optimized deposition voltage needs to be applied as different precursors go through reduction at different potential ranges. For instance, in the deposition of  $\text{Ge}_2\text{Sb}_2\text{Te}_5$ ,  $[\text{SbCl}_4]^-$  precursor is reduced most easily at -0.74 V, and  $[\text{TeCl}_6]^{-2}$  can be reduced to Te at  $-1.15 \sim -0.5 \text{ V}$ . On the contrary, reduction of Ge only occurs below -1.52 V. To insure the deposition of all three element to form  $\text{Ge}_2\text{Sb}_2\text{Te}_5$ , the deposition potential is set to be -1.75 V [57].

The above examples demonstrate that electrochemical deposition has the ability to synthesize both chalcogenides, and halides. It is a cheaper, faster and more controllable method in semiconductor synthesis field and fills the gaps where compound semiconductors with well-controlled stoichiometry and abrupt substrate-film interface cannot be obtained by other common methods, such as codeposition and vapor phase epitaxy.

## (a) Oxides

Functional metal oxides have always been the focus of both fundamental research and device applications. For instance, Potassium doped Barium bismuthate  $Ba_{1.x}K_xBiO_{3+y}$  (BKBO) has the highest superconducting transition temperature among copper and iron free superconductors [58]; ferromagnetic material,  $Fe_3O_4$ , exhibiting

spin-dependent charge transport property can be useful in giant magnetoresistance devices [59,60];  $Cu_2O$  is a p-type semiconductor with a large exciton binding energy [61] and negative differential resistance feature [62]; Cubic bismuth oxide ( $\delta$ -Bi<sub>2</sub>O<sub>3</sub>) has the highest known oxide ion mobility, which can be applied in fuel cells and sensors [63]. These oxides are appealing for device applications due to their intrinsic properties, but yet, we need to minimize grain boundary and other defects to further improve device performance and stability.

Zhang et al. [64], demonstrated a proof-of-concept for reversing the non-wettability of oxide on metal surface. They achieved epitaxial growth of Yttria-stablised zirconia (YSZ) nanoparticles on rough surface of Ni in a solid-oxide electrolysis cell. Porous Ni/YSZ was used as cathode and YSZ was used as solid electrolyte. During electrodeposition, Y<sup>3+</sup> and Zr<sup>4+</sup> ions obtained electrons and were reduced on the cathode side. In high-temperature gas environment, these reduced Y and Zr atoms diffused from Ni/YSZ interface to Ni grains. When they reach the Ni/gas interface, they were oxidized again under higher oxygen partial pressure and form observed YSZ nano-islands on Ni grains. HRTEM (Fig. 14) image demonstrated well-bonded YSZ nanoparticles with cubic symmetry on Ni grains with epitaxial relation of  $(-220)_{YSZ}//(0-20)_{Ni}$ with 3 % lattice mismatch. So electrochemical deposition can be used to prepare heterogeneous joining at micro-nanoscale of non-wetting oxide/metal system. Such heterojunctions formed between dissimilar materials are promising in energy and catalyst applications.

Enthusiasm in searching for high-temperature superconductors has never faded. Since Cava et al. [65] first synthesized a single phase perovskite  $Ba_{0.6}K_{0.4}BiO_3$  exhibiting a superconducting transition temperature of 29.8 K in 1988, many researchers employed various methods

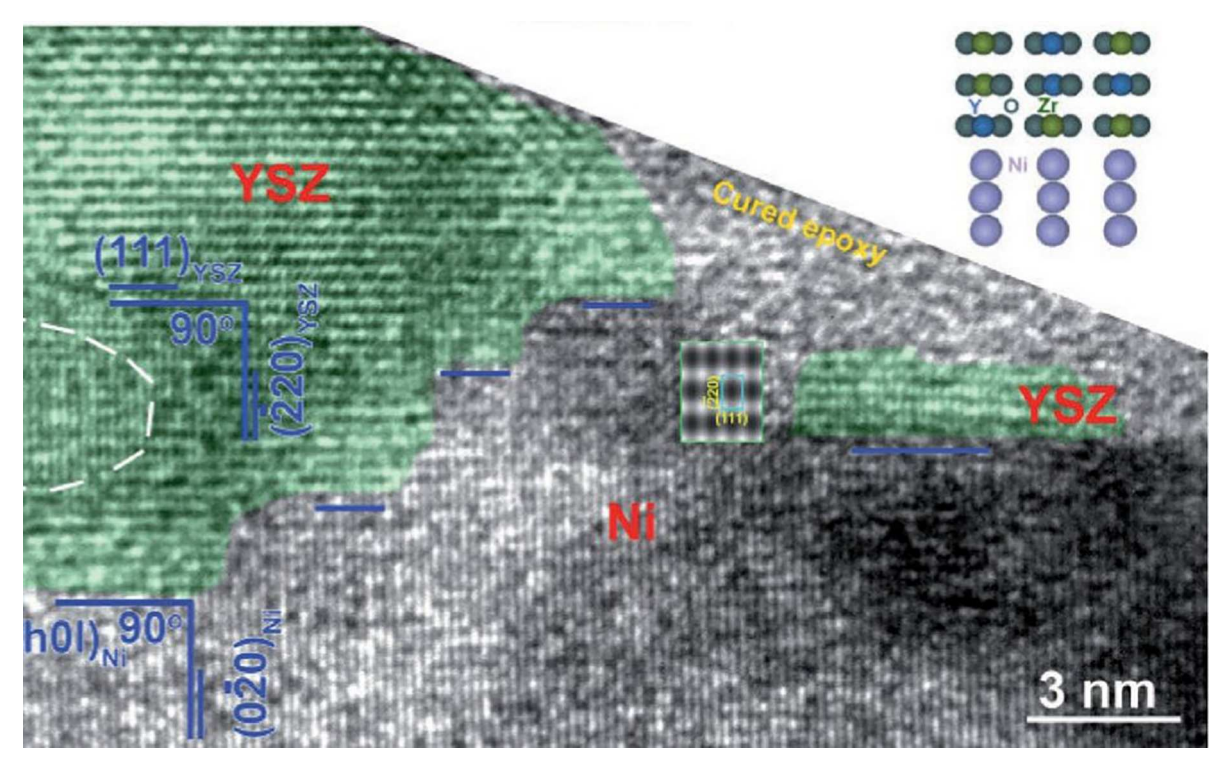


Fig. 14. HRTEM image of two epitaxially grown YSZ nanoparticles. Inset: interfacial crystallographic model. The white dashed line marks a Ni nanocrystal within the YSZ nanoparticle. (Adapted with permission from ChemElectroChem, 1 (2014) 520–523.).

to further improve the crystal quality, and thus, superconducting transition temperature. In 1996, Shiryaev et al. [58] successfully prepared superconductor  $Ba_{1.x}K_xBiO_{3+y}$  (0.32 $\leq$ x $\leq$ 0.53) (BKBO) on (100) $_c$  orientated  $BaBiO_3$  and  $Ba_{0.8}K_{0.2}BiO_3$  substrates through liquid-phase epitaxy in electrochemical cell. The electrochemical deposition is conducted in KOH melt containing  $Bi_2O_3$ , BaO and  $H_2O$  with various molar ratios. The average growth rate was measured to be 1–4  $\mu m/h$ . Good registry between BKBO film and  $BaBiO_3$  substrate was confirmed by the back-reflections Laue photography.

Besides being a low-cost and relatively easy to control synthesis method, electrochemical deposition also has the ability to grow materials in non-equilibrium phases due to its low deposition temperature. Switzer et al. [63], successfully obtained epitaxial high-temperature cubic polymorph of bismuth oxide,  $(\delta\text{-Bi}_2O_3)$ .  $\delta\text{-Bi}_2O_3$  is known for its high oxide ion mobility and it is an ideal material for applications in fuel cells, oxygen sensor, and oxygen pumps. In their experiment, the black  $\delta\text{-Bi}_2O_3$  film was electrochemically deposited at 65 °C onto Au (110), (100), (111) planes with strong out-of-plane and in-plane orientation and high structure perfection. The epitaxy relations were shown by Azimuthal x-ray diffraction scans as in Fig. 15(a)–(c) and the interface atom registry model is shown in Fig. 15(d)–(f). This work demonstrated that epitaxial growth can be achieved even the lattice mismatch is large. It also revealed the possibility of depositing other non-equilibrium material phases by electrochemical deposition method.

## (a) Organics

Organic materials appear in widely used devices, such as light-emitting diodes, field-effect transistors, solar batteries and so on. These organic alternative devices can be thinner, lighter and more flexible than their inorganic counterparts. Especially, conjugated polymers with well organized structure and morphology play a key role in determining the performance of these devices. Although electrochemistry has been a conventional method to prepare conjugated polymers for several decades [66,67], it is difficult to achieve deposition of well-organized polymer in molecular scale onto a substrate. Ren et al.

[18] and Sakaguchi et al. [19] realized epitaxy growth of conjugated polymers on single crystal substrate through electrochemical deposition from aqueous solutions.

Large area highly-ordered poly(3-hexylthiophene) (P3HT) on highlyordered isotactic polypropylene (i-PP) by epitaxial crystallization was achieved by Ren et al. [18]. The polymerization was realized by electrochemical process where monomers in the electrolyte were being electrochemically oxidized and formed polymer thin film on electrode through coupling reactions on the electrode surface. This process is schematically shown in Fig. 16a. In order to analyze the crystal structure and alignment of P3HT on i-PP, grazing incidence X-ray diffraction (GIXD) measurement was conducted. Together with FTIR and Raman results, they concluded that epitaxially crystallized P3HT had its bc-plane in contact with i-PP substrate with c-axis parallel to the draw direction of the i-PP film as shown in Fig. 16b and c. Thus, conjugated polymer thin film with well-defined crystal structure and molecular arrangement with respect to substrate can be obtained by electropolymerization, which can be a powerful method in preparing active layers in organic optoelectronic devices.

Sakaguchi et al. [19] also employed electropolymerization in preparing epitaxial high density single conjugated-polymer, polythiophene wires as long as 75 nm on Au (111) surface. Pulse voltage was used to conduct step-by-step electropolymerization of monomers from electrolyte. By this approach, they received epitaxial nanowire structures. They also concluded that the single-polythiophene wires formed on Au electrode was by surface propagation of polymer on the electrode surface. The experiment result shows potential applications of electropolymerization method to mass-production of molecular scale conjugated-polymer devices.

In summary, epitaxial electrochemical deposition stands as a transformative approach in semiconductor fabrication. It has ushered in a new era where precise control, low-temperature operation, and the creation of sharp interfaces are paramount. This versatile technique has broken free from the constraints of high-temperature processes, providing a cost-effective and efficient means of producing semiconductor materials.

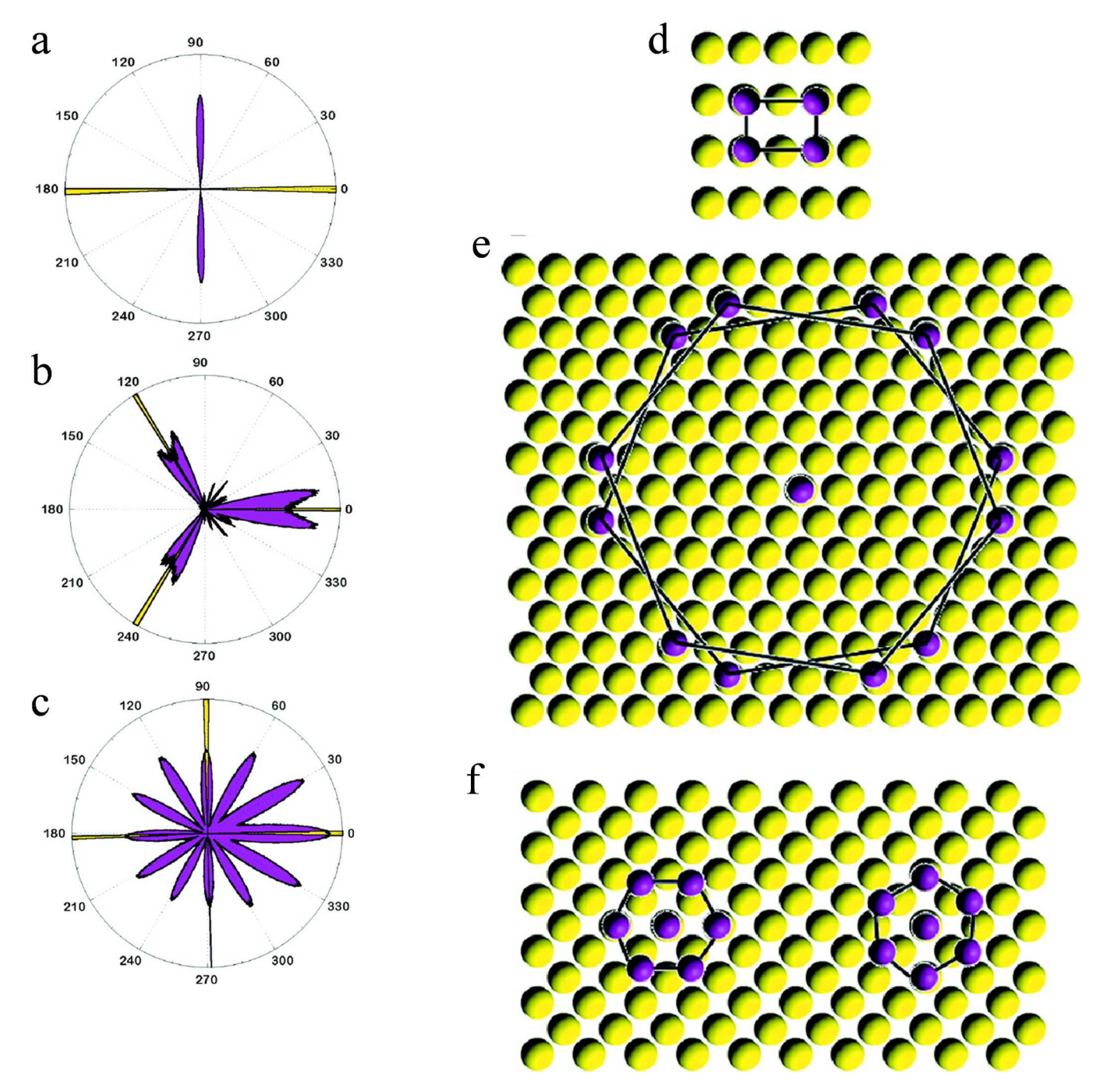


Fig. 15. Azimuthal x-ray diffraction scans probing the in-plane orientation of  $\delta$ -Bi<sub>2</sub>O<sub>3</sub> films deposited onto (a) Au(110), (b) Au(111), and (c) Au(100) single-crystal substrates; (d-f) Interface models for epitaxial growth of δ-Bi<sub>2</sub>O<sub>3</sub> on (d) Au(110), (e) Au(111), and (f) Au(100). The Au substrate atoms are yellow, and the Bi atoms of Bi<sub>2</sub>O<sub>3</sub> are purple. (Adapted with permission from Science 284 (5412), 293–296.).

Through its application to element semiconductors, compound semiconductors, oxides, and organic materials, epitaxial electrochemical deposition has demonstrated its remarkable adaptability across various material classes. From the growth of epitaxial germanium (Ge) films on silicon (Si) substrates to the precise control offered by electrochemical atomic layer epitaxy for compound semiconductor thin films, it has expanded the boundaries of what is achievable in semiconductor science. Moreover, the synthesis of functional metal oxides and the formation of heterogeneous junctions reveal the depth of its potential in energy and catalyst applications. In the organic realm, the epitaxial growth of conjugated polymers on single crystal substrates has opened up new vistas for highly organized and well-defined polymer

thin films, paving the way for innovative organic optoelectronic devices.

## Conclusions

This work reviews the capability of electrochemical epitaxy in preparing the thin film and nanostructure forms of a wide range of materials, such as metals, element and compound semiconductors, oxides, and organic polymers on appropriate substrates. Compared to molecular beam epitaxy, pulsed laser epitaxy and other vapor phase epitaxy approaches, electrochemical epitaxy is operated at relatively low temperature, so structures such as heteroepitaxial junctions that tend to be deteriorated by atom diffusion under high temperature can be fabricated

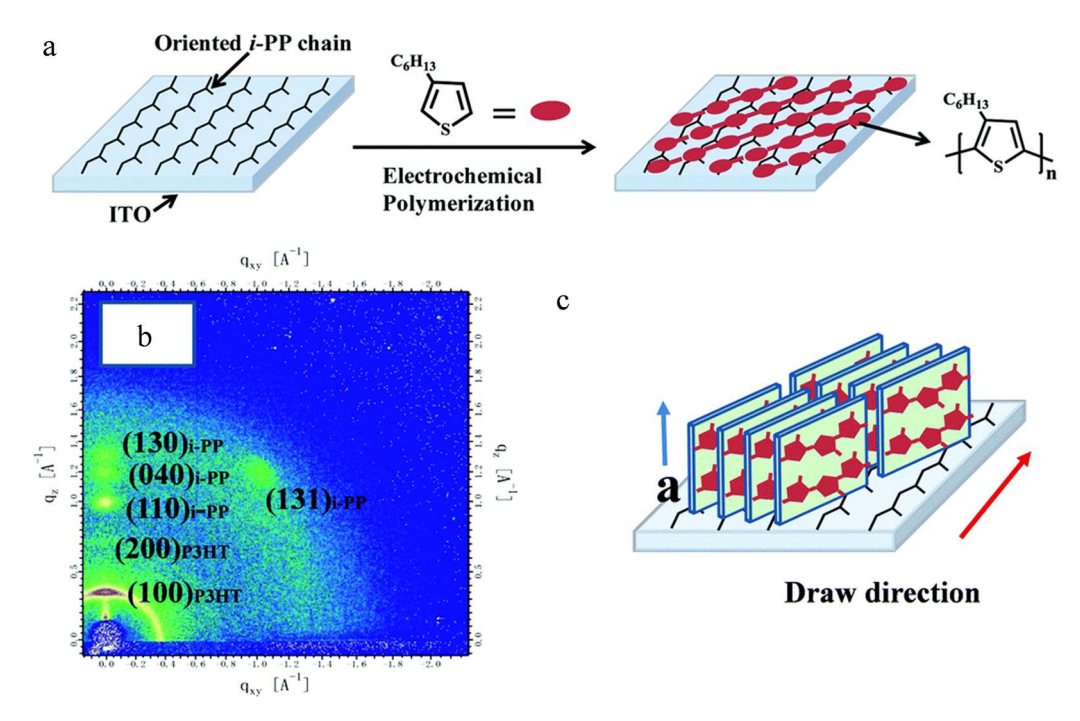


**Fig. 16.** (a) Schematic illustration of epitaxially electrochemical deposition of P3HT; (b) A grazing incidence X-ray diffraction (GIXD) 2D map obtained for deposited P3HT on the highly oriented i-PP. The 2D map is recorded for the incident X-ray beam oriented perpendicularly to the draw direction of i-PP. (c) Proposed structural ordering. (Adapted with permission from Chemical communications, 52 (2016) 10,972–10,975.).

with high crystal quality. Additionally, at low temperature, metastable phases may be synthesized following Ostwald rule of stages. Further, the use of electrochemical potential can conveniently manipulate the valence states of the metals which can not be simply done at vacuum conditions. Successful synthesis of superconducting BKBO film by electrodeposition at 240 °C and high-temperature phase of cubic  $\delta\textsc{-Bi}_2\textsc{O}_3$  at 65 °C are good examples to demonstrate the possibility of obtaining high/intermediate oxidation states not accessible at ambient oxygen atmosphere. Lastly, the relatively cheap and fast process of electrodeposition is a big advantage for technological mass-production. It is our hope that this review can serve as a guideline for future exploration of epitaxial growth of emerging materials including novel halides and chalcogenides.

## **Declaration of Competing Interest**

The authors declare that they have no known competing financial interests or personal relationships that could have appeared to influence the work reported in this paper.

# Acknowledgements

J.S. thanks NSF for the financial support under award no. of 2031692 and 2024972.

#### References

- H.A. Jehn, PVD and ECD-competition, alternative or combination? Surf. Coat. Technol. 112 (1999) 210–216.
- [2] J.W. Dini. Electrodeposition: the materials science of coatings and substrate, Noyes Publications, 1993, p. 141.
- [3] A. Gangulee, The structure of electroplated and vapor-deposited copper films, J. Appl. Phys. 43 (1972) 867.
- [4] A. Gangulee, Structure of electroplated and vapor-deposited copper films. II. effects of annealing, J. Appl. Phys. 43 (1972) 3943.
- [5] J.W. Dini, Defect structure, mophorlogy and properties of deposits, the minerals, Met. Mater. Soc. (1995) 369.
- [6] D.J. Willis, C. Hammond, Structure of chromium deposits from plating solutions containing trivalent and hexavalent chromium, Mater. Sci. Technol. 2 (1986) 630.

- [7] L.H. Esmore, The electrodeposition of high purity chromium, Trans. Inst. Met. Finish. 57 (1979) 57.
- [8] E.S. Chen, Improved electrodeposited low contraction chromium, U.S. Army research & development command, Technical Report ARLCB-TR-82009, (1982).
- [9] J.W. Dini, Properties of coatings: comparison of electroplated, physical vaper deposited, chemical vapor deposited and plasma sprayed coatings, Mater. Manuf. Process. 12 (3) (1997) 437–472.
- [10] B.M. Basol, E.S. Tseng, D.S. Lo, U.S. Pat 4,629,820 (1986).
- [11] G. Mu, Chemical bath deposition and electrodeposition of epitaxial semiconductor materials for application in photovoltaic deivces, dissertation, Missouri University of Science and Technology, (2010).
- [12] H.A. Jehn, PVD and ECD-competition, alternative or combination? Surf. Coat. Technol. 112 (1999) 210–216.
- [13] R. Winand, Electrodeposition of metals and alloys-new results and perspectives, Electrochim. Acta 39 (1994) 1091.
- [14] S. Beauvais, A.M. Huntz, G. Moulin, L. Beylat, J.J. Blechet, The oxidation mechanism of chromium coating by a continuity CO<sub>2</sub> laser constant temperature, Corros. Sci. 35 (1993) 1225.
- [15] K. Trethewey. Chamberlain, corrosion for science and engineering, 2nd ed., Longman, 1995.
- [16] D.W. Suggs, I. Villegas, B.W. Gregory, J.L. Stickney, Formation of compound semiconductors by electrochemical atomic layer epitaxy, J. Vac. Sci. A 10 (1992) 886–891.
- [17] R.M. Penner, Hybrid electrochemical: chemical synthesis of quantum dots, Acc. Chem. Res. 33 (2000) 78–86.
- [18] Z. Ren, X. Zhang, H. Li, X. Sun, S. Yan, A facile way to fabricate anisotropic P3HT films by combining epitaxy and electrochemical deposition, Chem. Commun. 52 (2016) 10972–10975.
- [19] H. Sakaguchi, H. Matsumura, H. Gong, Electrochemical epitaxial polymerization of single-molecular wires, Nat. Mater. 3 (2004) 551–557.
- [20] N.K. Mahenderkar, Q. Chen, Y. Liu, A.R. Duchild, S. Hofheins, E. Chason, J. Switzer, Epitaxial lift-off of electrodeposited single-crystal gold foils for flexible electronics, Science 355 (2017) 1203–1206.
- [21] P. Prod'homme, F. Maroun, R. Cortès, P. Allongue, Electrochemical growth of ultraflat Au (111) epitaxial buffer layers on H-Si(111), Appl. Phys. Lett. 93 (2008), 171901
- [22] S. Warren, P. Prod'homme, F. Maroun, P. Allongue, R. Cortès, C. Ferrero, T.L. Lee, B.C.C. Cowie, C.J. Walker, S. Ferrer, J. Zegenhagen, Electrochemical Au deposition on stepped Si (111)-H surfaces: 3D versus 2D growth studied by AFM and X-ray diffraction, Surf. Sci. 603 (2009) 1212–1220.
- [23] W. Schindler, J. Kirschner, Ultrathin magnetic films: electrochemistry versus molecular-beam epitaxy, Phys. Rev. B 55 (1996) R1989.
- [24] Y. Liu, D. Gokcen, U. Bertocci, T.P. Moffat, Self-terminating growth of Platinum films by electrochemical deposition, Science 338 (2012) 1327–1330.
- [25] M. Li, Q. Ma, W. Zi, X. Liu, X. Zhu, S. Liu, Pt monolayer coating on complex network substrate with high catalytic activity for the hydrogen evolution reaction, Sci. Adv. 1 (2015) 8.

- [26] Y. Kim, J. Kim, D. Vairavapandian, J.L. Stickney, Platinum nanofilm formation by EC-ALE via redox replacement of UPD copper: studies using in-situ scanning tunneling microscopy, J. Phys. Chem. B 110 (2006) 17998–18006.
- [27] K. Sieradzki, S.R.N. Dimitrov, Electrochemical defect-mediated thin-film growth, Science 284 (1999) 138–141.
- [28] H.J. Pauling, G. Staikov, K. Jüttner, Layer-by-layer formation of heterostructured ultra-thin films by UPD and OPD of metals, J. Electroanal. Chem. 376 (1994) 179–184.
- [29] R. Vasilic, N. Dimitrov, Epitaxial growth by monolayer-restricted galvanic displacement, Electrochem. Solid State Lett. 8 (2005) C173.
- [30] J.X. Wang, B.M. Ocko, R.R. Adzic, Overpotential deposition of Ag monolayer and bilayer on Au(111) mediated by Pb adlayer underpotential deposition/stripping cycles, Surf. Sci. 540 (2003) 230–236.
- [31] S.R. Brankovic, N. Dimitrov, K. Sieradzki, Surfactant mediated electrochemical deposition of Ag on Au (111), Electrochem. Solid State Lett. 2 (1999) 443–445.
- [32] S. Hwang, I. Oh, J. Kwak, Electrodeposition of epitaxial Cu(111) thin films on Au (111) using defect-mediated growth, J. Am. Chem. Soc. 123 (2001) 7176–7177.
- [33] L.T. Viyannalage, R. Vasilix, N. Dimitrov, Epitaxial growth of Cu on Au(111) and Ag(111) by surface limited redox replacements-an electrochemical and STM study, J. Phys. Chem. C 111 (2007) 4036–4041.
- [34] M. Dietterle, T. Will, D.M. Kolb, The initial stages of copper deposition on Ag(111): an STM study, Surf. Sci. 342 (1995) 29–37.
- [35] M. Dietterle, T. Will, D.M. Kolb, The initial stages of Cu electrodeposition on Ag (100): an in situ STM study, Surf. Sci. 396 (1998) 189–197.
- [36] T. Will, M. Dietterle, D.M. Kolb, The initial stages of electrolytic copper deposition an atomic view, Nanoscale Probes Solid Liquid Interface (1995) 137–162.
- [37] F.Y. Yang, K. Liu, K. Hong, D.H. Reich, P.C. Searson, C.L. Chien, Large magnetoresistance of electrodeposited single-crystal Bismuth thin films, Science 284 (1999) 1335–1337.
- [38] U. Cohen, R.A. Huggins, Silicon epitaxial growth by electrodeposition from molten fluorides, J. Electrochem. Soc. 123 (1976) 381–383.
- [39] T.A. Sorenson, K. Varazo, D.W. Suggs, J.L. Stickney, Formation of and phase transitions in electrodeposited tellurium atomic layers on Au(111), Surf. Sci. 470 (2001) 197–214.
- [40] J. Demuth, E. Fahrenkrug, L. Ma, T. Shodiya, J.I. Deitz, T.J. Grassman, S. Maldonado, Electrochemical liquid phase epitaxy (ec-LPE): a new methodology for the synthesis of crystalline group IV semiconductor epifilms, J. Am. Chem. Soc. 139 (2017) 6960–6968.
- [41] D.W. Suggs, J.L. Stickney, Studies of the structures formed by the alternated electrodeposition of atomic layers of Cd and Te on the low-index planes of Au, Surf. Sci. 290 (1993) 362–374.
- [42] L.P. Colletti, B.H. Flower, J.L. Stickney, Formation of thin films of CdTe, CdSe, and CdS by electrochemical atomic layer epitaxy. J. Electrochem.Soc. 145 (1998) 5.
- [43] T.E. Lister, L.P. Colletti, J.L. Stickney, Electrochemical formation of CdSe monolayers on the low index planes of Au, Isr. J. Chem. 37 (1997) 287–295.
- [44] T.E. Lister, J.L. Stickney, Formation of the first monolayer of CdSe on Au (111) by electrochemical ALE, Appl. Surf. Sci. 107 (1996) 153–160.
- [45] M. Foresti, G. Pezzatini, M. Cavallini, G. Aloisi, M. Innocenti, R. Guidelli, Electrochemical atomic layer epitaxy deposition of CdS on Ag (111): an electrochemical and STM investigation, J. Phys. Chem. B 102 (1998) 7413–7420.
- [46] M. Cavallini, M. Facchini, C. Albonetti, F. Biscarini, M. Innocenti, F. Loglio, E. Salvietti, G. Pezzatini, M.L. Foresti, Two-dimensional self-organization of CdS ultra thin films by confined electrochemical atomic layer epitaxy growth, J. Phys. Chem. C 111 (2007) 1061–1064.
- [47] G. Pezzatini, S. Caporali, M. Innocenti, M.L. Foresti, Formation of ZnSe on Ag(111) by electrochemical atomic layer epitaxy, J. Electroanal. Chem. 475 (1999) 164–170.
- [48] R. Vaidyanathan, J.L. Stickney, S.M. Cox, S.P. Compton, U. Happek, Formation of In2Se3 thin films and nanostructures using electrochemical atomic layer epitaxy, J. Electroanal, Chem. 559 (2003) 55–61.
- [49] V. Venkatasamy, M.K. Mathe, S.M. Cox, U. Happek, J.L. Stickney, Optimization studies of HgSe thin film deposition by electrochemical atomic layer epitaxy (EC-ALE), Electrochim. Acta 51 (2006) 4347–4351.

- [50] M.K. Mathe, S.M. Cox, V. Venkatasamy, U. Happek, J.L. Stickney, Formation of HgSe Thin films using electrochemical atomic layer epitaxy, J. Electrochem. Soc. 152 (2005) C751.
- [51] R. Vaidyanathan, J.L. Stickney, U. Happek, Quantum confinement in PbSe thin films electrodeposited by electrochemical atomic layer epitaxy (EC-ALE), Electrochim. Acta 49 (2004) 1321–1326.
- [52] W. Zhu, J.Y. Yang, X.H. Gao, S.Q. Bao, X.A. Fan, T.J. Zhang, K. Cui, Effect of potential on bismuth telluride thin film growth by electrochemical atomic layer epitaxy, Electrochim. Acta 50 (2005) 4041–4047.
- [53] T. Öznülüer, Ü. Demir, Formation of Bi<sub>2</sub>S<sub>3</sub> thin films on Au(111) by electrochemical atomic layer epitaxy: kinetics of structural changes in the initial monolayers, J. Electrochem. Soc. 529 (2002) 34–42.
- [54] H. Kang, R. Liu, K. Chen, Y. Zheng, Z. Xu, Electrodeposition and optical properties of highly oriented γ-CuI thin films, Electrochim. Acta 55 (2010) 8121–8125.
- [55] A.T. Hubbard, D.G. Peters, Electrochemistry in thin layers of solution, Crit. Rev. Anal. Chem. 3 (1973) 201.
- [56] B.W. Gregory, J.L. Stickney, Electrochemical atomic layer epitaxy (ECALE), J. Electroanal. Chem. 300 (1991) 543–561.
- [57] P.N. Bartlett, S.L. Benjamin, C.H. Groot, A.L. Hector, R. Huang, A. Jolleys, G. P. Kissling, W. Levason, S.J. Pearce, G. Reid, Y. Wang, Non-aqueous electrodeposition of functional semiconducting metal chalcogenides: Ge<sub>2</sub>Sb<sub>2</sub>Te<sub>5</sub> phase change memory, Mater. Horiz. 2 (2015) 420.
- [58] S.V. Shiryaev, S.N. Barilo, N.S. Orlova, D.I. Zhigunov, A.S. Shestac, V.T. Koyava, V. I. Gatalskaya, A.V. Pushkarev, V.M. Pan, V.F. Solovjov, Epitaxial growth of single crystal films of Ba<sub>1-x</sub>K<sub>x</sub>BiO<sub>3+y</sub> superconductor, J. Cryst. Growth 172 (1997) 296, 403
- [59] M.P. Nikiforov, A.A. Vertegel, M.G. Shumsky, J.A. Switzer, Epitaxial electrodeposition of Fe<sub>3</sub>O<sub>4</sub> on single-crystal Au(111), Adv. Mater. 12 (2000) 1351–1353.
- [60] T.A. Sorenson, S.A. Morton, G.D. Waddill, J.A. Switzer, Epitaxial electrodeposition of Fe<sub>3</sub>O<sub>4</sub> thin films on the low-index planes of gold, J. Am. Chem. Soc. 124 (2002) 7604–7609.
- [61] R. Liu, E.W. Bohannan, J.A. Switzer, F. Oba, F. Ernst, Epitaxial electrodeposition of Cu<sub>2</sub>O films onto InP(001), Appl. Phys. Lett. 83 (2003) 1944–1946.
- [62] E.W. Bohannan, M.G. Shumsky, J.A. Switzer, Epitaxial electrodeposition of copper (I) oxide on single-crystal gold(100), Chem. Mater. 11 (1999) 2289–2291.
- [63] J.A. Switzer, M.G. Shumsky, E.W. Bohannan, Electrodeposited ceramic single crystals, Science 284 (1999) 293–296.
- [64] W. Zhang, M. Chen, L. Theil Kuhn, J.R. Bowen, J.J. Bentzen, Electrochemistry unlocks wettability: epitaxial growth of oxide nanoparticles on rough metallic surfaces, ChemElectroChem 1 (2014) 520–523.
- [65] R.J. Cava, B. Batlogg, J.J. Krajewski, R. Farrow, L.W. Rupp, A.E. White, K. Short, W.F. Peck, T. Kometani, Superconductivity near 30K without copper: the Ba<sub>0.6</sub>K<sub>0.4</sub>BiO<sub>3</sub> perovskite, Nature 332 (1998) 814–816.
- [66] G. Tourillon, F. Garnier, New electrochemically generated organic conducting polymers, J. Electroanal. Chem. 135 (1982) 173–178.
- [67] F. Garnier, G. Tourillon, J.Y. Barraud, H. Dexpert, First evidence of crystalline structure in conducting polythiophene, J. Mater. Sci. 20 (1985) 2687–2694.
- [68] K. Reddy, M.M. Maqableh, B.J. Stadler, Epitaxial Fe(1-x)Gax/GaAs structures via electrochemistry for spintronics applications, J. Appl. Phys. 111 (2012) 07E502.
- [69] J.L. Stickney, S.D. Rosasco, D. Song, M.P. Soriaga, A.T. Hubbard, Superlattices formed by electrodeposition of silver on iodine-pretreated Pt(111); studies by LEED, Auger spectroscopy and electrochemistry, Surf. Sci. 130 (1983) 326–347.
- [70] A.T. Hubbard, J.L. Stickney, S.D. Rosasco, M.P. Soriaga, D. Song, Electrodeposition on a well-defined surface: silver on Pt(111)(√7×√7)R19.1° –I, J. Electroanal. Chem. 150 (1983) 165–180.
- [71] R. Vaidyanathan, S.M. Cox, U. Happek, D. Banga, M.K. Mathe, J.L. Stickney, Preliminary studies in the electrodeposition of PbSe/PbTe superlattice thin films via electrochemical atomic layer deposition (ALD), Langmuir 22 (2006) 10590–10595.